Soils and Rocks

An International Journal of Geotechnical and Geoenvironmental Engineering

www.soilsandrocks.com

ISSN 1980-9743
ISSN-e 2675-5475

Three-dimensional numerical analysis of the effect of foundation stiffness on soil-structure interaction

Nathani Zampirolli[1#], Aldo Durand Farfán[1], Paulo César de Almeida Maia[1]

Article

Keywords
Soil-structure interaction in tall buildings
Three-dimensional numerical model
Continuous flight auger pile

Abstract
Stiffness-related geometric characteristics are closely linked to the performance of structural systems. The influence of foundation stiffness on the soil-structure interaction (SSI) mechanism was investigated by numerical modeling of different building foundations. Numerical tools (PLAXIS 3D and TQS/CAD) were used for decoupling analyses of the interaction between the structural components. Results obtained from instruments installed in a building case study were used to refine the numerical calculations. Linear elastic constitutive models and beam elements were useful in reducing computational processes and ensuring study feasibility. The simulation results provided a satisfactory representation of field observations. Interaction between piles and the environment governs the relationship between foundation stiffness and uniform settlement. Rigid pile groups are achieved with greater pile length, diameter and spacing. This study highlights the different effects of pile geometric parameters on loading and unloading rates in pillars, demonstrating that the SSI mechanism is more sensitive to less rigid foundations, particularly those with greater pile embedment. It was concluded that numerical simulations to predict settlement as realistically as possible require understanding and selecting the most appropriate model and type of calculation.

1. Introduction

In engineering projects, supports are traditionally considered rigid and fixed, while the foundation is calculated independently of the frame, considering constant loads. Analyzing the superstructure without considering the foundation (or vice-versa) disregards forces, bending moments and settlement resulting from soil-structure interaction (SSI) (Thangaraj & Ilamparuthi, 2010). Thus, it is vital to analyze the structural system considering the soil, foundation and superstructure as a compatible unit. In fact, the different parts of the structure interact and are directly associated with the system's ability to absorb and redistribute additional stress among the structural elements. This redistribution of stresses in the structure is known as soil-structure interaction (SSI), a mechanism directly linked to the performance of the construction project. Frantziskonis & Breysse (2003) reported that the performance of the structural system is also closely linked to the geometric and stiffness characteristics of the foundation. SSI may change the realistic behavior of a pile group and as such, the proper design of pile foundations must consider the interaction between the building frame, soil and pile group (Koteswara et al., 2020). This study aimed to investigate the relationship between SSI and foundation stiffness, using PLAXIS 3D and TQS/CAD for numerical modeling of the interaction between the structural elements.

Current research on SSI is fundamentally based on formulating and using numerical methods, such as the finite element method (FEM), which makes it possible to simulate soil heterogeneity, considering stratified layers and the physical and geometric nonlinearity of the structure. Buragohain et al. (1977), Ingle & Chore (2007), Chore & Ingle (2008), Chore et al. (2009) & Chore et al. (2010) investigated pile-supported building frames using FEM to assess the effect of different foundation parameters on the superstructure. Their research emphasizes the importance of interaction between structural system components and the need to consider pile stiffness and flexibility in structural analysis. Dode et al. (2014) evaluated the effect of the spacing, diameter and number of piles in a pile group on superstructure response. Kiran & Madhav (2015) discussed the effect of parameters such as the relative stiffness of two soil layers and pile length-to-diameter ratio (L/D) on settlement behavior for a single pile under axial loading. Koteswara et al. (2020) used FEM and scale experiments to analyze the effect of a building frame on the behavior of a pile group in terms of pile settlements, cap rotation, head deflection and bending moment, by varying the pile spacing and L/D ratio, as well as the relative density of the sand bed. The study demonstrated

[#]Corresponding author. E-mail address: nathanizamp@gmail.com
[1]Universidade Estadual do Norte Fluminense Darcy Ribeiro, Laboratório de Engenharia Civil, Campos dos Goytacazes, RJ, Brasil.

Submitted on May 27, 2024; Final Acceptance on September 2, 2024; Discussion open until February 28, 2025.
https://doi.org/10.28927/SR.2024.000424

that bearing capacity increases with the L/D ratio in both the single pile and pile group, especially with a rise in L, and emphasizes the importance of considering the effect of interaction between the subsoil, foundation and superstructure on pile group behavior. Rasi et al. (2020) considered SSI in FEM analyses to assess the effect of variations in foundation stiffness on settlement and concluded that greater stiffness resulted in uniform settlement. Bhartiya et al. (2020) studied pile groups and piled rafts with different geometries and configurations to determine the stiffness of these components and corresponding settlement. The authors conducted parametric studies and found that pile-soil interaction depends on pile length and diameter, as well as the elastic properties of the soil and foundation system. They also demonstrated that pile group settlement depends on the stiffness of individual piles which, in turn, depends on structural stiffness k_p (Equation 1) and stiffness resulting from pile-soil interaction (I_{ps}). This is related to pile group stiffness K_F by Equation 2, which includes both the structural and geotechnical components of stiffness. Interaction between single piles and the soil depends on the pile L/D and Young's modulus of the soil and pile.

$$k_p = \frac{A_p E_p}{Lp} \tag{1}$$

$$K_F = k_p I_{ps} \tag{2}$$

where A_p is the cross-sectional area of the pile, and E_p and Lp are its Young's modulus and length, respectively.

Studies in the literature focus on piles (single or groups) under different types of stress, with most investigations of the SSI mechanism analyzing stress in the superstructure (forces and moments). There are few experimental studies, particularly cases of real construction projects, that consider the effect of SSI and its relationship with foundation stiffness. In this context, the present study aimed to demonstrate the relationship between foundation stiffness and SSI in a real building. To that end, a parametric study was performed based on 3D linear-elastic numerical analysis via FEM, in conjunction with structural matrix analysis. For the building studied here, settlement readings from 46 pillars throughout the construction period were analyzed (Prellwitz, 2016). Numerical models validated by back-analysis with field results made it possible to implement different foundations based on pile L/D values within ± 10% of the diameter (D) and length (L) of the piles originally designed for the building. SSI was incorporated into the analyses via iterative decoupling, with the foundation and superstructure modeled in PLAXIS 3D and TQD/CAD software, respectively.

2. Numerical models

The structure modeled is a multi-family residential building with 196 autonomous units and 19 floors. In ascending order, it starts at the ground floor, divided into a parking garage and reception area, followed by two floors (G1 and G2) consisting of parking garages, and another floor divided into the PUC (leisure area) and a parking garage. Next, there are 14 standard floors and finally the roof slab, where the roof and access to the water tank are located. Construction time is measured in days and starts at 0 days, when the foundation is poured. Construction of the 5th slab was completed in 316 days and the 10th, 14th and 19th slabs, including the enclosing masonry, were completed on days 435, 498 and 621, respectively. After completion of the enclosing masonry, 100% of the total load of the construction was applied to the supports.

The decoupled approach adopted in the present study required constructing two-part numerical models consisting of the superstructure and foundation. The superstructure was simulated in TQS/CAD (Figure 1) and the foundation and soil mass in PLAXIS 3D. A three-dimensional model was selected in order to include the expected group effects for the foundation in the analyses. Leite et al. (2023) studied the group effect and concluded that it is significant in displacements, demonstrating increased settlement due to the overlapping stress bulbs of the piles and neighboring pile groups.

Figure 2 shows the floor plan of the ground floor pillars of the building and its different sectors under mean foundation loading. The building body consists of a reinforced concrete frame on a foundation of 18-meter-deep continuous flight auger piles 500mm in diameter in a heterogeneous sedimentary soil mass typical of the Campos dos Goytacazes region in Rio de Janeiro state, Brazil. The pillars of the body of the building were monitored and the pillars around the perimeter of the parking garage were not monitored and are not part of this study.

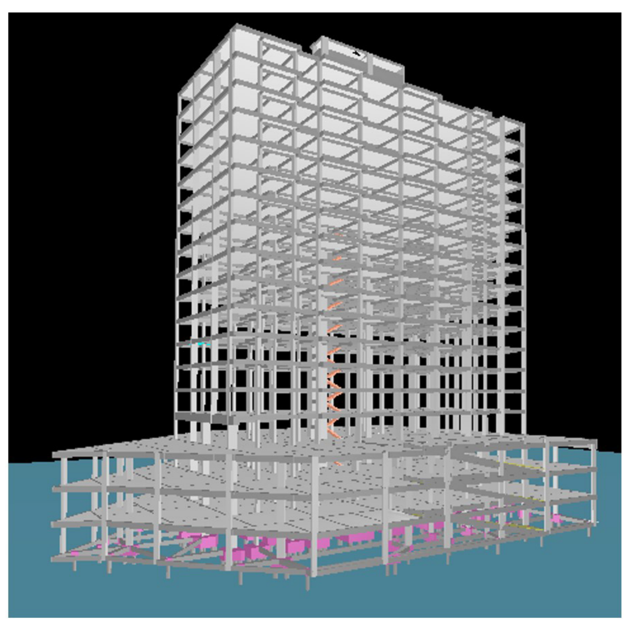

Figure 1. 3D model of the superstructure in TQS©.

Interpretations of standard penetration test (SPT) data were input into the numerical model of the foundation, which was calibrated based on results from settlement monitoring instruments in a study by Prellwitz (2016). Calibration details are presented in item 3.1. In order to monitor building settlement during construction, the author instrumented all the pillars of a 20-floor multifamily building in Campos dos Goytacazes, Rio de Janeiro state, Brazil, based on the principle of communicating vessels (see Prellwitz, 2015).

The three-dimensional FEM model was constructed to include the representative soil stratigraphy. The model boundaries were large enough to prevent the limits of the modeled from influencing the results of the problem. The structural elements were modeled considering "embedded beam" type elements for the piles and "plate" type for the capping blocks, and the contact between the soil and structural element considering an interface parameter whose value corresponds to that indicated in the technical literature (equal to 1, according to Brinkgreve & Shen, 2011). Although the program does not directly consider the effects of structural element installation, the assumed interface resistance (R_{inter}) value of one imposes a rough interface on the model, a reasonable premise since the continuous helix pile is cast in situ. This results in a lower load transfer from the pile to the soil when compared to slightly rough or smooth interfaces. The input parameters of the concrete elements are based on laboratory test results for the same building under study, reported by (Maia et al., 2019) and presented in Table 1.

3. Numerical analysis

The numerical models were used in calculations to study the effect of foundation stiffness on SSI mechanisms. This study was conducted via parametric analysis combined with iterative decoupling to assess the iterative mechanism between the structure and the calibrated model of the foundation.

Initially, stratigraphy in the numerical model was proposed based on the result of the field investigation carried out for the foundation (SPT holes), as mentioned in the previous item. The typical soil profile is shown in Figure 3. The probes indicated a surface layer of silty clay with N_{SPT} values of fewer than 10 blows, followed by a dense approximately 4-meter-thick sand layer (average N_{SPT} of 15 blows), a layer of soft clay up to 2 m thick, and a hard clay layer whose N_{SPT} increased with depth, reaching 40 blows. Figure 3 also shows the geotechnical parameters used as input in the model. Details on these values are provided below.

The superstructure model presented in Figure 1 was used to calibrate the geotechnical parameters, considering the construction sequence. The foundation was modeled using PLAXIS 3D. Calibration was performed by back-analysis, using the pillar settlements measured in the field as reference.

Table 1. Pile input parameters (Maia et al., 2019).

E (GPa)	v	γ (kN/m³)
14.8	0.11	20.69

Legend: see List of symbols and abbreviations.

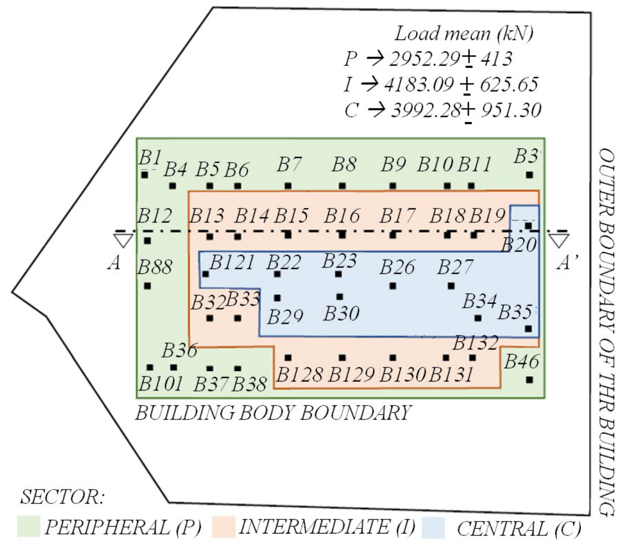

Figure 2. Floor plan of the 46 ground floor pillars of the building, its sectors under mean loading and AA cross-section.

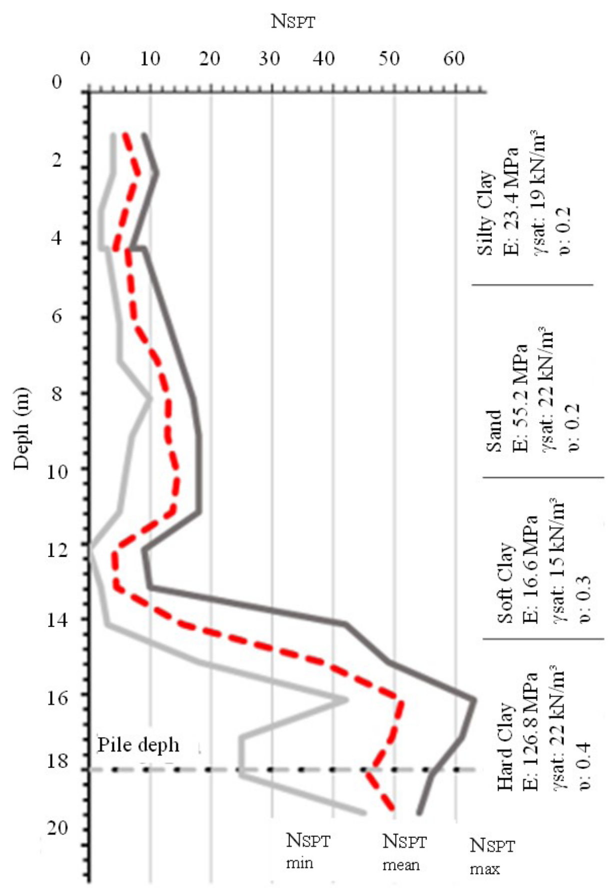

Figure 3. Equivalent soil profile.

Initially, parameters were determined using semi-empirical correlations based on N_{SPT} (Decourt, 1995; Marangon, 2009; Ortigão, 2007).

Next, the estimated loads were applied in line with the construction sequence. Load estimation for each loading stage of the pillars was computed using TQS/CAD software with the SISEs module (TQS Informática, 2019). Each loading stage corresponds to the concreting of a building slab. Given the considerable number of loading stages (19 slabs) and the lengthy processing time needed to include all the stages, only 4 were considered for numerical modeling (5th, 10th, 14th, and 19th slabs).

Several numerical simulations were performed at each processing stage, thus refining the geotechnical parameters until the displacements in the numerical model were consistent with the measured values. For refinement, the geotechnical parameters of the model were avaried within the confidence interval obtained through the spatial variation of the properties of each layer shown in Figure 3.

The calibration results are presented in Figure 4, which shows settlement progression for each processing stage. It is evident that the proposed modeling process provided a reliable estimate of foundation behavior in terms of trend and magnitude, assuming the order of magnitude of the values obtained. The calibration results also demonstrated that adopting field tests traditionally used in geotechnical projects (SPT) combined with back-analysis of in-situ settlement readings is a reasonable approach in numerical modeling. The foundation model consisted of an equivalent medium for the soil mass, and the linear elastic constitutive law was adopted for each soil layer, as recommended by Poulos (1989) and Mandolini & Viggiani (1997).

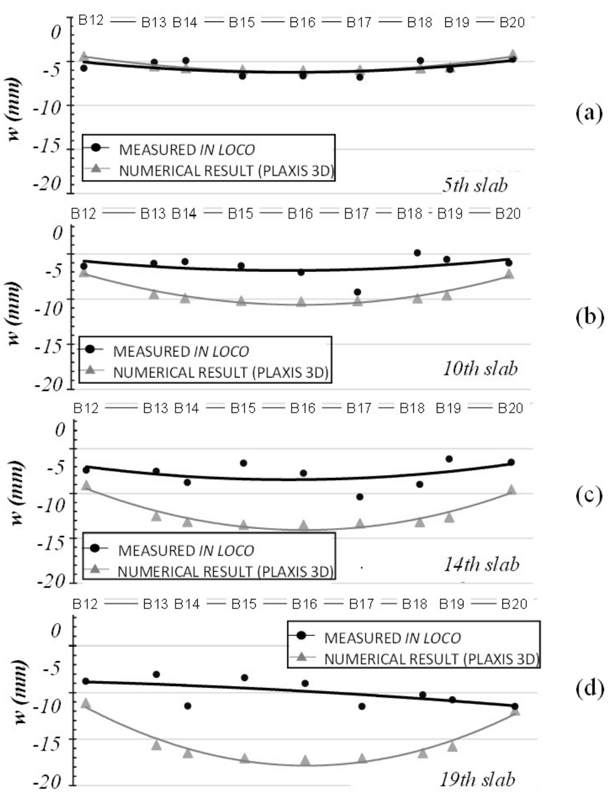

Figure 4. Foundation settlement profiles (AA cross-section) for the stages in which the (a) 5th, (b) 10th, (c) 14th, (d) and 19th slabs were constructed.

In Figure 4, the settlements obtained by the numerical model are overestimated. This is fundamentally justified by the simplifications inherent in the modeling process. The 3D model via FEM requires high computational effort for geometrically sophisticated models or the adoption of sophisticated constitutive models. The equivalent soil mass adopted made modeling feasible without considerably compromising deformation tendency and behavior in the foundation. As such, adopting equivalent stratigraphy and modeling with a linear elastic constitutive equation is reasonable for this case study, which, despite numerical limitations inherent to the process, made it possible to consider the group effect of the piles in determining stresses in the foundation.

3.1 Iterative decoupling methodology

Given the calibrated numerical models, a methodology was adopted to consider soil-structure interaction between the decoupled models and evaluate the effects of the proposed foundation stiffness.

The iterative decoupling methodology applied to determine loads and settlement with SSI effects for the building was based on the process described by Aoki & Cintra (2004), with the spring coefficient incorporated into the model in line with the methodology of Chamecki (1954). For each analysis, a numerical routine was devised (illustrated in Figure 5) that enabled the calculation of the loads and settlement associated with the building pillars. In this routine, SSI is considered when the settlements are induced in the TQS model. The spring coefficient introduced in the TQS/CAD model is determined based on the settlement obtained in the PLAXIS 3D model. This procedure is iterative until settlement converges between the models.

In Figure 5, the process begins with the matrix model of the superstructure (TQS/CAD) that calculates the load on the pillars in each stage of building construction. Initially, the hypothesis of zero displacements (settlements equal to zero) was considered. The load stages were simplified to four stages corresponding to the 5th, 10th, 14th and 19th slabs. In this respect, the nonlinear static calculation yields the reactions of each pile (Q) in each stage, which are applied to the foundation (FEM model). This produces the respective settlement values (w) at the top of the blocks that form the base of the pillars, thus making it possible to determine pillar base stiffness. This pillar stiffness corresponds to the vertical spring coefficient k (kN/m), which is equivalent to the ratio between the load (Q) and settlement (w).

A sequence of interactions is established for each load stage considered, whereby the stiffness calculated for each pillar is input into the matrix model, which provides new pillar reactions due to the redistribution of structural stress. The process is repeated until the difference between settlement values obtained in two subsequent iterations is less than a mean error of 2%. In the present study, four to six iterations were needed for the settlement values to converge. Stress redistribution among the structural elements as loading progresses is one of the main effects of SSI. As a result, uniform settlement and smooth foundation settlement profiles are expected (Gusmão, 1990). Indeed, iterative decoupling prompted a tendency to uniform settlement on the settlement vs. time curve in the final load stages of construction.

3.2 Parametric study

Different pile geometries referred to as 'cases' were compiled for the parametric study of the foundation, with each case analyzed individually in a specific FEM model. The calculation routine presented in Figure 5 was used in each case to ensure that SSI was considered in the assessment of the effect of foundation stiffness.

Table 2 presents the geometry and respective stiffnesses for each case and the corresponding structural stiffnesses of the foundation (k_p) given by Equation 1, since SSI depends on pile length and diameter as well as the elastic properties of the soil and foundation system. Each case established resulted in different pile length-to-diameter ratios (*L*/*D*). Diameter (*D*) and length (*L*) were adopted at ± 10% of the measurements of the piles originally designed for the project. Case zero corresponds to the real geometry of the construction project.

4. Study of the effect of foundation stiffness on SSI mechanisms

4.1 Settlement sensitivity

For each case in Table 2, the rate of settlement progression according to load increase was assessed and expressed in number of construction days in Figure 6. The figures indicate an inverse relationship between the length-to-diameter ratios *L/D* and settlement, that is, for a same diameter, piles that are less slender produce greater settlement (case 1), while their more slender counterparts create less settlement (case 2). Cases 1 and 2 were also constant (less sensitive) during the loading process, unlike when diameter varied (cases 3 and 4), since foundation settlement is sensitive to this parameter, particularly in the early load stages. When pile length is varied, the expected increase and decrease in $w_{AVERAGE}$ is 1.072 and 0.089%, respectively, with 2.96 and 3.14% for pile diameter changes. Taken together with foundation analysis, this indicates that settlement is more sensitive to changes in pile length regardless of whether settlement tends to decline due to changes in geometry. This tendency stabilizes as the construction project progresses, unlike that observed when diameter variations are used to achieve more or less settlement in building projects. As the number of building floors increases, settlement tends to progressively decline with

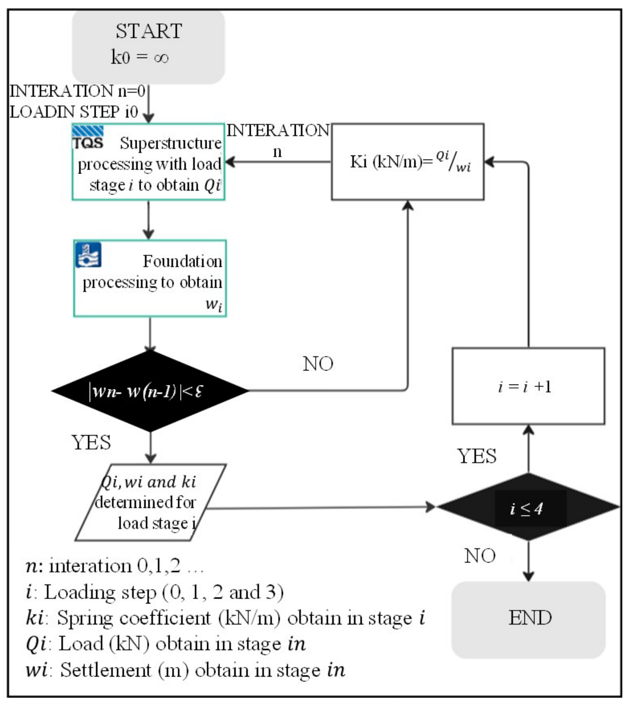

Figure 5. Iterative decoupling methodology.

Table 2. Foundation geometry for the *cases* considered.

Case	*D* (m)	*L* (m)	*L*/*D*	k_p x 10^8 (kN/m)
0	0.5	18.0	36.0	1.61
1	0.5	16.2	32.4	1.79
2	0.5	19.8	39.5	1.46
3	0.45	18.0	40.0	1.30
4	0.55	18.0	32.7	1.95

Legend: see List of symbols and abbreviations.

the reduction in pile diameter. Finally, the increase in pile proportions is associated with greater bearing capacity, with piles consequently producing less settlement (Case 2 and 4).

4.2 Sensitivity of foundation stiffness (K_F)

Analysis of the foundation as a single system considered pile group stiffness K_F, given by the ratio between working load (Q) and displacement (w) of the pile group (Equation 3).

$$K_F = \frac{Q}{w}\left(kN/m\right) \tag{3}$$

Figure 7 presents the $K_{F\,AVERAGE}$ of all the pillars in the building, along with the progression of this parameter for the cases considered.

In general, foundation stiffness increases as construction advances and tends to stabilize in the final stages of building. This is justified by the greater soil strength caused by increased confinement of the adjacent soil mass. The effects of changes in pile geometric parameters are evident.

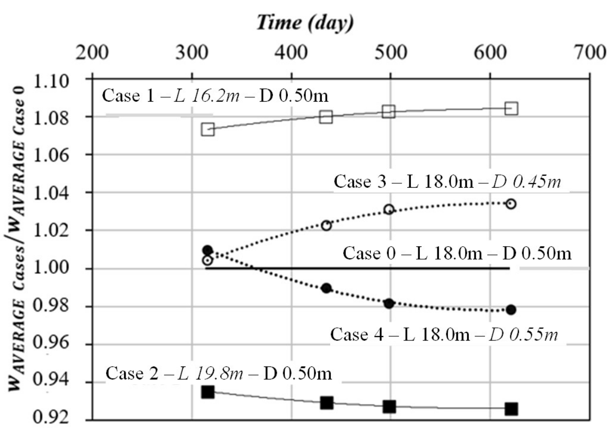

Figure 6. Normalized settlement over time for each case analyzed.

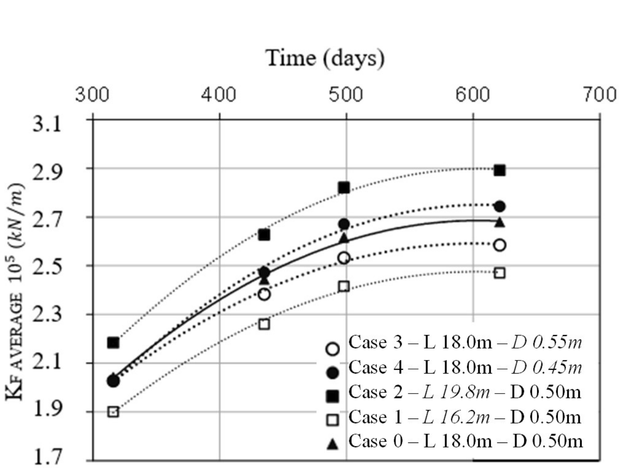

Figure 7. $K_{F\,AVERAGE}$ progression for the cases considered.

The lower settlement depicted in Figure 7 corresponds to higher K_F values; thus, longer and wider piles result in stiffer pile groups. This demonstrates that foundation stiffness is strongly related to the pile L or D adopted in the foundation design. Length sensitivity is greater than that observed in pile diameter analysis, making it consistent with the findings of Zampirolli et al. (2022).

4.3 Soil-structure interaction (SSI)

One of the main effects of SSI is load redistribution in the structure. The absolute settlement factor (AR) proposed by Gusmão (1990), given by Equation 4, makes it possible to analyze the effects of SSI, more specifically of load redistribution, while the *iso-AR* curves make it easier to visualize the areas on the floor plan of the ground floor pillars subjected to this effect. Figure 8 shows the spatial location of the pillars in the floor plan and the *iso-AR* curves. Pillars with a higher load level are situated in the center of the floor plan and those with lower working loads around the edge (peripheral sector), with unloading ($AR > 1$) evident in the former and overloading in the latter. This result confirms the technical literature that predicts the tendency to unloading in the most and overloading in the least loaded pillars, due to the SSI mechanism (Gusmão, 2006).

$$AR = \frac{w}{w_{AVERAGE}} \qquad \begin{array}{l} AR > 1 \rightarrow Unloading \\ AR < 1 \rightarrow Overloading \end{array} \tag{4}$$

Changes in D and L and, consequently, in the structural stiffness of the element, have a similar effect on AR. Figure 9 demonstrates that the sensitivity of this factor to pile stiffness is around 1% for geometry variations (L or D). When settlement decreases due to the use of longer piles, overloading in the latter ($AR < 1$).

Overloaded pillars are stiffer than their unloaded counterparts, a characteristic observed consistently across all construction stages and for both geometric variations (length, L, and diameter, D). The influence of pile L/D ratios is evident in the overloading curves (Figures 9c and 9d), with lower L/D values resulting in smaller settlements and higher values larger settlements.

By contrast, in the unloading curves (Figures 9a and 9b), smaller L/D ratios produced larger settlements and higher values smaller settlements.

It is important to discuss an interesting fact regarding AR tendencies, as shown in Figure 9 and described in the literature (Gusmão, 1990). According to the literature, AR tends to one at the end of building construction due to the expected increase in building stiffness, which acts predominantly to minimize settlement dispersion. In Figure 9, the AR coefficient curve is close to 0.90, on average, at the end of construction. This value can be improved by

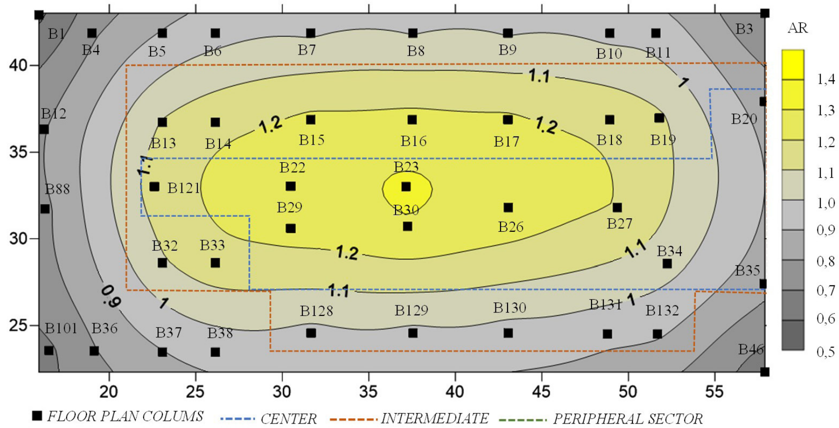

Figure 8. Iso-*AR* curves for *case* 0.

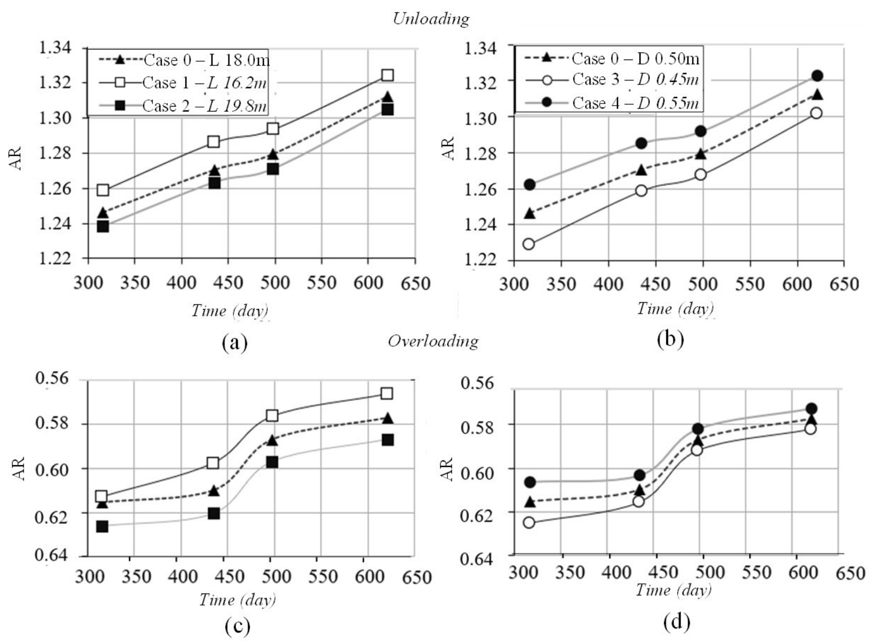

Figure 9. Progression of the *AR* coefficient of the pillars according to the construction sequence; (a) and (c) behavior due to the variation in pile length "*L*" (b) and (d) diameter "*D*".

adjusting the tolerance in the decoupling approach adopted to include SSI in the analyses (shown in Figure 5). It is important to note that the numerical model makes it possible to simulate behavior observed in the field, identifying pillars with unloading ($AR > 1$, which have a higher load level, in the central sector) and overloading ($AR < 1$, with lower working loads, in the peripheral sector), in line with the technical literature (Gusmão, 1990).

Barros (2005) proposed load redistribution assessment in pillars using the load redistribution coefficient (*FQ*), given by Equations 5 and 6, which depict load variation between pillars as a value between -1 and 1, with *FQ* values from –1 to 0 indicating unloading, 0 to 1 overloading and $FQ = 0$ (zero) no SSI. Where R_{ISE} is the reaction at the support point of pillar i, obtained based on the flexibilized model, and R_{IND} the reaction calculated considering the fixed pillars. The author also suggested that foundation behavior be assessed in relation to building geometry via the *CV* coefficient and that equivalent foundation characteristics be considered. Thus, for the case studied here, it is pertinent to compare the *CV* of isolated areas of the system (central, intermediate and peripheral sectors in Figure 2).

$$FQ = \frac{R_{ISE} - R_{IND}}{R_{IND}} \quad \text{For } R_{IND} \;\; R_{ISE} \tag{5}$$

$$FQ = \frac{R_{ISE} - R_{IND}}{R_{ISE}} \quad \text{For } R_{IND} < R_{ISE} \tag{6}$$

In general, changes in average foundation stiffness do not affect the expected SSI trend but influence the magnitude of load redistribution among the pillars and the level of settlement dispersion in the building (*FQ* and *CV*, respectively). In fact, regardless of foundation stiffness, the central and intermediate pillars tend to unloading and those in the peripheral sector, overloading.

Figure 10 illustrates the relationship between load redistribution and the degree of absolute settlement uniformity. The *FQ* and *CV* coefficients were obtained for each stage of building construction and for each sector of the floor plan (I – intermediate, C – central e P – peripheral).

Figure 10 shows unloading in the central and intermediate pillars. However, load redistribution across the pillars in these sectors exhibits specific behavior, with practically constant unloading (3.0 to 3.4%) and increasing settlement dispersion in the intermediate section, whereas the opposite is expected in the center. Increasing unloading associated

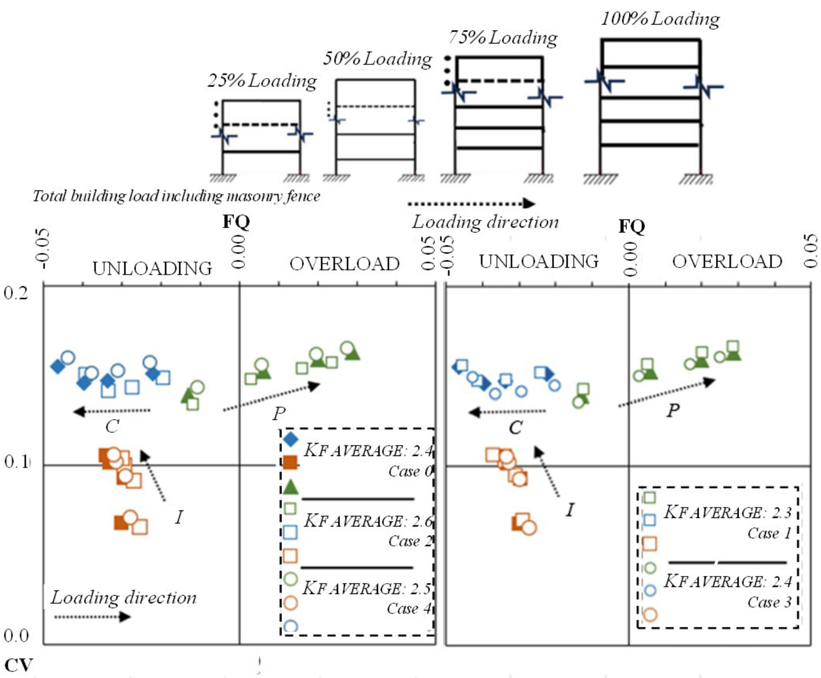

Figure 10. CV_{MEAN} vs. FQ for the building sectors and cases considered.

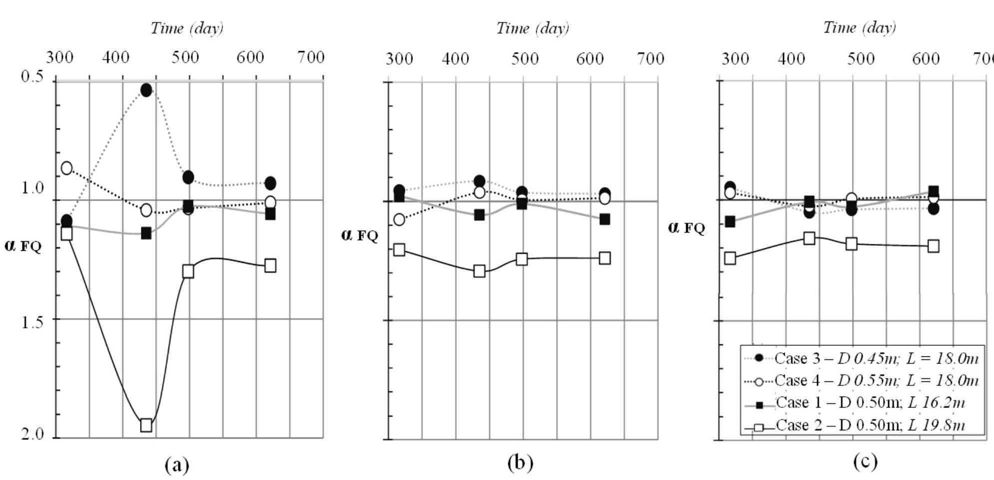

Figure 11. Progression of normalized FQ for each sector analyzed for the (a) central; (b) intermediate and (c) peripherical sectors.

with constant settlement CV_{MEAN} (around 15%) in the center of the building can be justified by the restrictions imposed on the pillars by the frame, which acts predominantly by reducing settlement dispersion. While the location of pillars is not necessarily determinant in SSI effects, the load on these structural elements plays a decisive role in this mechanism.

In general, changes in average foundation stiffness do not affect the expected SSI trend but influence the magnitude of load redistribution among the pillars and the level of settlement dispersion in the building (*FQ* and *CV*, respectively).

Indeed, regardless of foundation stiffness, the central and intermediate pillars tend to unloading and those in the peripheral sector, overloading.

Increased foundation stiffness promotes greater *FQ* and *CV*, particularly for pillars in the center of the building, albeit with a more moderate effect in the remaining sectors.

When diameter is the cause of varying foundation stiffness (cases 3 and 4), greater *CV* fluctuations are expected, while changes in L (cases 1 and 2) have a greater effect on *FQ*. This is more pronounced in the peripheral and central sectors, which seems to suggest that foundation stiffness and its effect on SSI differ according to the characteristics of the element (structural stiffness) the size and diameter of pile embedment. Quantitative assessment of the effect of the structural stiffness of the foundation on load redistribution is shown in Figure 11, demonstrating the proportional increase or decrease in load redistribution in the pillars from each sector, via α_{FQ} given by Equation 7, as building construction progresses. The further the α_{FQ} value is from one, the greater the expectation that the change in stiffness proposed by the case will contribute to load redistribution. However, when α_{FQ} is close to one, variations in foundation stiffness are expected to have little influence on *FQ*.

$$\alpha_{FQ} = \frac{FQ_{CASE\,n}}{FQ_{CASE\,0}}, n = 1,\ 2,\ 3\ and\ 4 \tag{7}$$

In general, the effect of changes in foundation stiffness on *FQ* are more evident in the initial stages of construction, especially in peripheral pillars. In fact, this phase is more susceptible to SSI effects because the structure exhibits less bending stiffness, which is conferred as the number of floors increases (Gusmão, 2006). *FQ* variation rates are higher along the periphery than in the remaining sectors, which may be associated with the greater load redistribution in the less loaded pillars. Since the peripheral pillars are more susceptible to SSI effects, with higher overloading rates, in this case study foundation stiffness changes are expected to have a greater influence on SSI in this sector.

FQ is more sensitive to variations in L, especially in case 2, regardless of the section in which the pillars are located. The largest variations in *FQ* are expected at low foundation *kp* values (cases 2 and 3). This confirms that *FQ* is more sensitive to less rigid foundations, particularly those with greater pile embedment.

In general, the intermediate sector obtained the smallest *FQ* variation rates when *kp* changes. Pillars in the intermediate section of the building are therefore less susceptible to the effects of foundation stiffness in terms of the SSI mechanism, unlike that observed in less loaded pillars.

5. Conclusion

The iterative methodology proposed here uses successive simulations of structural calculations (TQS/CAD) and stress-strain analysis (PLAXIS), which proved to be an effective approach in understanding loading and unloading rates in foundations for a 20-floor building with 46 pillars. This enabled parametric analyses to investigate the relationship between the structural stiffness of the foundation and the SSI mechanism.

Iterative decoupling also made it possible to analyze the sensitivity of foundation stiffness to changes in pile diameter and length. Greater pile embedment produced a more significant settlement reduction when compared with an increase in the contact area of the pile in this study case for these specific soil conditions, in line with the technical literature (Reul & Randolph, 2004).

Loads greater than 75% cause greater soil confinement, evident in the stable stiffness behavior of the foundation system. Moreover, foundation stiffness is directly related to how the pile interacts with the soil and not necessarily to the structural stiffness of the foundation. In fact, uniform settlement in the building depends on this interaction, since it was found that the use of more rigid parts does not necessarily result in uniformity. Fundamentally, the type of geometric parameter associated with stiffness (*D* and *L*) is a decisive factor in analysis.

This study concluded that the pursuit of low settlement in construction projects should be carefully analyzed, since pile geometric parameters have different effects on unloading and overloading rates in the pillars.

Acknowledgements

This research was funded by FAPERJ – Fundação de Amparo à Pesquisa do Estado do Rio de Janeiro. The authors would like to thank the researchers who provided the data referring to the work analyzed and the researchers who collaborated with the development of this research, Marta Prellwitz (PhD), Géssica Marquezini (M.Sc.) and Lorena Leite (M.Sc).

Declaration of interest

The authors have no conflicts of interest to declare. All co-authors have analyzed and approved the content of the manuscript and there is no financial interest to report.

Authors' contributions

Nathani Zampirolli: conceptualization, data curation, formal analysis, investigation, methodology, validation, visualization, writing – original draft. Aldo Durand Farfán: conceptualization, data curation, supervision, validation, writing – review and editing. Paulo César de Almeida Maia: supervision, validation, writing – review and editing.

Data availability

The datasets generated analyzed in the course of the current study are available from the corresponding author upon request.

List of symbols and abbreviations

k_p	Geometric coefficient of the piles
s	Spacing between piles in a block
w	Absolute settlement of the pillars
AR	Settlement factor
CV	Coefficient of variation of absolute settlement
D	Pile diameter
E	Young's modulus
FEM	Finite element method
FQ	Coefficient of load redistribution in the pillars
I_{ps}	Pile-soil interaction
K	Vertical spring coefficient
K_F	Stiffness of the foundation system
L	Pile length
N_{SPT}	Number of blows in the SPT
Q	Load
R_{inter}	Interface resistance
SSI	Soil-structure interaction
SPT	Standard penetration test
ULS	Ultimate limit state
α_{FQ}	Load redistribution factor in the pillars
γ	Soil specific weight
v	Poisson's ratio

References

Aoki, N., & Cintra, J.C. (2004). *Notas de aula disciplina SGS-404 "Fundações"*. São Carlos: Departamento de Geotecnia, Universidade de São Paulo.

Barros, R.A. (2005). *Previsão e controle de recalques durante a construção de edifícios* [Dissertação de mestrado]. Laboratório de Engenharia Civil, Universidade Estadual do Norte Fluminense Darcy Ribeiro.

Bhartiya, P., Chakraborty, T., & Basu, D. (2020). Settlement estimation of piled rafts for initial design. *Journal of Geotechnical and Geoenvironmental Engineering*, *146*(2), 04019127. http://doi.org/10.1061/(ASCE)GT.1943-5606.0002195.

Brinkgreve, R.B.J., & Shen, R.F. (2011). *Structural elements and modeling excavations in plaxis*. Power Point Presentation File.

Buragohain, D.N., Raghavan, N., & Chandrasekharan, V.S. (1977). Interaction of frames with pile foundation. In *Proceedings of International Symposium on Soil-structure Interaction* (pp. 109-115), Roorkee, India.

Chamecki, S. (1954). Consideração da rigidez da estrutura no cálculo dos recalques da fundação. In *Anais do I Congresso Brasileiro de Mecânica dos Solos* (pp. 35-80, Vol. 1), Porto Alegre, RS.

Chore, H.S., & Ingle, R.K. (2008). Soil-structure interaction analyses of pile supported building frame. *ASEAN Journal on Science and Technology for Development*, *25*(2), 457-467. http://doi.org/10.29037/ajstd.276.

Chore, H.S., Ingle, R.K., & Sawant, V.A. (2009). Building frame-pile foundation-soil interactive analysis. *Interaction and Multiscale Mechanics*, *2*(4), 397-411. http://doi.org/10.12989/imm.2009.2.4.397.

Chore, H.S., Ingle, R.K., & Sawant, V.A. (2010). Building frame-pile foundation-soil interaction analysis: a parametric study. *Interaction and Multiscale Mechanics*, *3*(1), 55-79. http://doi.org/10.12989/imm.2010.3.1.055.

Decourt, L. (1995). Prediction of load-settlement relationships for foundations on the basis of standard penetration test. In *Ciclo de Conferencias Internationale Leonardo Zeevaert* (pp. 85-104). Mexico: UNAM.

Dode, P.A., Chore, H.S., & Agrawal, D.K. (2014). Interaction analysis of a building frame supported on pile groups. *Coupled Systems Mechanics*, *3*(3), 305-318. http://doi.org/10.12989/csm.2014.3.3.305.

Frantziskonis, G., & Breysse, D. (2003). Influence of soil variability on differential settlements of structures. *Computers and Geotechnics*, *30*(3), 217-230. http://doi.org/10.1016/S0266-352X(02)00062-9.

Gusmão, A.D. (1990). *Estudo da interação solo-estrutura e sua influência em recalques de edificações* [Dissertação de mestrado]. Universidade Federal do Rio de Janeiro.

Gusmão, A.D. (2006). Desempenho de fundações de edifícios. In *Palestras XIII COBRAMSEG* (pp. 215-240), Curitiba.

Ingle, R.K., & Chore, H.S. (2007). Soil-structure interaction analysis of building frames: an overview. *Journal of Structural Engineering*, *34*(5), 201-209.

Kiran, K.V., & Madhav, M.R. (2015). Settlement of single granular pile at different depths. In *Indian Geotechnical Conference*. New Delhi: IGS.

Koteswara, V.R.P., Padavala, H., & Chennarapu, H. (2020). Experimental and numerical investigation of pile group with and without building frame subjected to axial load. *Indian Geotechnical Journal*, *50*(3), 473-484. http://doi.org/10.1007/s40098-019-00383-5.

Leite, L.S., Maia, P.C.A., & Farfán, A.D. (2023). Three-dimensional numerical analysis of the generalized group effect in monitored continuous flight auger pile groups. *Soils and Rocks*, *46*(2), e2023013722. http://doi.org/10.28927/SR.2023.013722.

Maia, P.C.A., Prellwitz, M.F., & Waked, L.V. (2019). Estimate of elastic modulus of continuous flight auger concrete. *Geotecnia*, 147, 27-40. .

Mandolini, A., & Viggiani, C. (1997). Settlement of piled foundations. *Geotechnique*, 47(4), 791-816. http://doi.org/10.1680/geot.1997.47.4.791.

Marangon, M. (2009). *Notas de "Aula de Tópicos em Geotecnia e Obras de Terra: estabilidade de taludes"* (30 p.). Juiz de Fora: UFJF.

Ortigão, J.A.R. (2007). *Introdução à mecânica dos solos dos estados críticos* (3ª ed., 374 p.). Rio de janeiro: Livros Técnicos e Científicos Editora Ltda.

Poulos, H. (1989). Pile behaviour: theory and application. *Geotechnique*, 39(3), 365-415. http://doi.org/10.1680/geot.1989.39.3.365.

Prellwitz, M.F. (2015). *Monitoramento de recalques por fotogrametria usando o princípio dos vasos comunicantes*. [Dissertação de mestrado]. Universidade Estadual do Norte Fluminense Darcy Ribeiro.

Prellwitz, M.F. (2016). *Aplicação de monitoramento de recalque para estimativa de parâmetro de interação solo-estrutura* [Doctoral thesis]. Laboratório de Engenharia Civil, Universidade Estadual do Norte Fluminense Darcy Ribeiro, Campos dos Goytacazes.

Rasi, J.R., Serafim, J.A., Mazer, W., & Broetto, J.F. (2020). Análise das reações nas estacas em bloco de concreto considerando a interação solo-estrutura. *Brazilian Journal of Development*, 6(6), 41410-41425. http://doi.org/10.34117/bjdv6n6-616.

Reul, O., & Randolph, M.F. (2004). Design strategies for piled rafts subjected to nonuniform vertical loading. *Journal of Geotechnical and Geoenvironmental Engineering*, 130(1), 1-13. http://doi.org/10.1061/(ASCE)1090-0241(2004)130:1(1).

Thangaraj, D.D., & Ilamparuthi, K. (2010). Parametric study on the performance of raft foundation with interaction of frame. *The Electronic Journal of Geotechnical Engineering*, 15, 1-18.

TQS Informática. (2019). *CAD/TQS: manual de início rápido* (31 p.). São Paulo: TQS Informática Ltda.

Zampirolli, N., Farfan, A.D., & Maia, P.C.A. (2022). Numerical analysis of the effect of pile group stiffness on settlement in sedimentary soil. In *Proceedings of 20th International Conference on Soil Mechanics and Geotechnical Engineerin* (pp. 1049-1054). Sydney, Australia.